Indian Journal of Biochemistry & Biophysics
Vol. 63, February 2026, pp. 145-152
DOI: 10.56042/ijbb.v63i2.20790

Optical properties of DNA-polydimethylsiloxane double layered structures

Gasparyan L, Simonyan V & Gasparyan F*
DNA-HIVE LLC, Rockville, MD, USA

Received 19 June 2025; *revised 30 June 2025*

To create nanoscale UV sensors and devices based on biomaterials, a detailed study of their optical properties and current transport mechanisms is necessary. In this paper, we study the optical properties of a bilayer structure containing DNA. The transfer matrix method is used. The analysis is performed considering both the real and imaginary parts of the refractive indices of both layers. Reflectance, transmittance, and absorptance spectra are determined. At the average values of the real and imaginary parts of the refractive indices of DNA absorptance passes through a maximum at 215-220 nm and a minimum at 250-260 nm. When considering the spectral distribution of the real and imaginary parts of the DNA refractive index, the absorbance shifts along the wavelength toward longer waves, passes through a minimum at 220 nm, and then through a maximum at 257 nm. The extremes of the absorptance shift to the long-wave region with an increase in the angle of incidence of the radiation. An attempt is made to explain the spectral behaviour of DNA absorptance and its dependence on the value of the imaginary part of DNA refractive index and the angle of incidence of the irradiation. Using the approximation method based on the spectral dependence of acceptance, a formula for the absorption coefficient of DNA is obtained. The acceptability of using the transfer matrix method for studying the optical parameters of organic materials with a complex refractive index is shown.

Keywords: Absorptance, Reflectance, Refractive index, Transfer matrix method

DNA is the main target of UV irradiation in both lower and higher organisms. DNA containing materials are attracting increasing attention and scientific interest for their application in optical nanoscale devices. Properties such as flexibility and complementary interaction with electronic structures recommended biomaterials for integration into several organic optical devices. Being renewable, biodegradable and environmentally friendly, biomaterials can lead to non-polluting technologies and effective cost reduction of the optical devices (biosensors, organic bioLEDs, bioFETs, bioLASERs, capacitors, photovoltaic devices, memory devices, amplifiers and non-linear optical modulators, *etc*.)[1-6]. DNA, RNA and nucleobases may soon become "building blocks" in the field of nanoelectronics and nanotechnology.

The results of the study of the optical properties of thin-film DNA complexes based on cetyltri-methylammonium (DNA-CTMA) applied to an optical elastomer substrate show their suitability for the creation of bio photonic devices[7]. The absorption of DNA-CTMA rapidly increases up to 270-280 nm, then rapidly decreases. A biosensor for detecting DNA hybridization *via* refractive index sensing has been demonstrated using a subwavelength grating waveguide[8]. By varying the RNA concentration and the precipitation process parameters, homogeneous continuous layers of solid RNA with thicknesses ranging from 30 to 46 nm were successively produced[9]. Starting from the irradiation wavelength of ~200 nm, the reflectance of DNA molecules decreases with increasing wavelength, passes through a minimum at ~228 nm, then increases, passes through a maximum at ~260 nm and drops to zero at ~310 nm[10]. The electronic spectrum of nucleobases shows a prominent absorption peak at 260 nm, a valley at 231 nm in the UV range, and a relatively strong absorption peak in the IR range[11]. With increasing angle of incidence of irradiation, the reflection decreases. The behavior of the absorptance of DNA molecules in various combinations with various substrates and in different combinations under different circumstances differs in minimum values at ~230 nm and maximum at ~260 nm[1,12-14]. At present, the technology for producing thin layers of DNA, RNA and nitrogenous bases is quite advanced. They can be prepared by various methods, including organic extraction, precipitation, laser ablation, silica-based purification and chromatographic methods, vacuum thermal evaporation and solution-based methods such as centrifugation and

*Correspondence:
E-mail: fgaspar@myyahoo.com

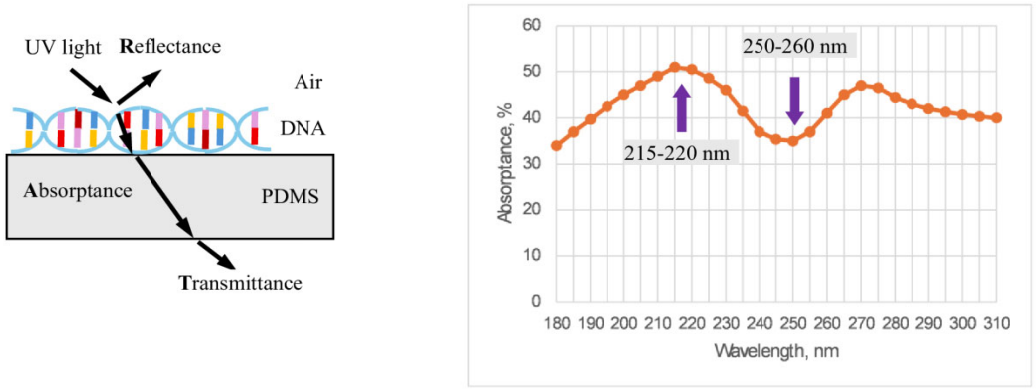

Graphical abstract

layer-by-layer precipitation[15-17]. Polydimethylsiloxane (PDMS) is often used for scientific research on structures with organic materials. PDMS has a low refractive index, weak absorption in the visible region, high thermal and chemical stability, and biocompatibility[18]. The low refractive index will allow us to achieve a noticeable difference between the refractive indices of the layers studied. It is also worth noting that PDMS can be prepared as a thin, separate layer[7].

Optimization of optical properties of multilayer thin-film structures containing organic materials depending on the wavelength and angle of incidence of irradiation, as well as many other purposes, is an interesting and promising scientific direction[19-21]. The main modeling methods commonly used in the field of subwavelength antireflection structures are the finite difference time domain method (FDTD), the finite element method (FEM), the rigorous coupled wave analysis or Fourier modal method (RCWA/FMM), and the transfer matrix method (TMM)[22,23]. TMM is one of the most powerful methods in modern theoretical physics. Typically, TMM was used to model the linear propagation of electromagnetic waves through a layered medium. The layered structure may consist of several thin-film materials with different thicknesses and different refractive indices. The task becomes more interesting from the point of view of the development of bioelectronics and biosensorics when organic material is used instead of layers. TMM has been successfully used to study the optical properties of complex multilayer structures to reduce reflection for solar cells[24], to study the wave transmission in one-dimensional structures and allows one to calculate band diagrams, reflection and transmission spectra, emission spectra[23], guided modes, and the modeling of porosity and thickness gradients[25].

This work is devoted to the theoretical study (modeling) of the optical properties of thin-layer DNA under UV-B irradiation. The TMM method will be used to study the features of the spectral dependencies of reflectance and absorptance of the thin-layer DNA/PDMS bilayer structure. The calculations are carried out considering both the real and imaginary parts of the reflective indices of both layers.

Optical parameters of DNA-PDMS Double Layered Structure

DNA stability is fundamental to the proper functioning and existence of living systems. Irradiation has an adverse effect on genome stability. UV-B irradiation (280–315 nm) and longwave part of irradiation UV-C (100-280 nm) is one of the important mechanisms that alter the normal state of life. Cells are constantly exposed to various environmental influences. Under their influence, genomic DNA is damaged, which poses a threat to their proper functioning.

Let us consider the optical properties (reflectance and transmittance) of a double layer structure: organic molecules (DNA)/substrate (PDMS). Figure 1 shows a schematic representation of the thin-layer DNA-PDMS bilayer structure we studied under UV irradiation. The substrate and the layer of DNA are characterized by the complex refractive indexes $\tilde{n}_1$ and $\tilde{n}_2$, correspondingly. In Figure 1, I_0 is the intensity of the incident irradiation, θ_0 is the angle of incidence, and R is the total reflectance from the surface. Within a two-layer structure, multiple reflections will occur from the interfaces between the layers. The angles of incidence of irradiation at the corresponding interlayer boundaries are denoted by θ_1, and θ_2, reflectances as R, R_1 and R_2, T denotes the transmittance, t_1 and t_2 are thicknesses of the layers, n_0 is the refractive index of the air, $\tilde{n}_1$ and $\tilde{n}_2$

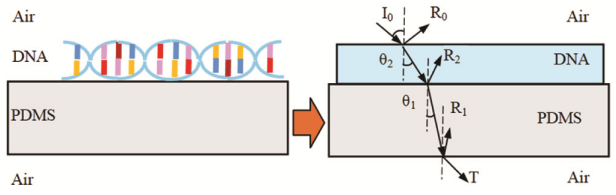

Fig. 1 — Double-layer DNA-PDMS structure under irradiation

are complex refractive indices and n_1, n_2, k_1, k_2 are real and imaginary parts of refractive indices of corresponding PDMS and DNA layers.

Based on the presented in Fig. 1 geometric construction with the use of TMM, the reflectance and transmittance of light irradiation through DNA/PDMS structure can be determined by setting the parameters of all the layers included in it. To calculate the absorption spectrum of DNA, it is necessary to consider the losses of irradiation in the layers of the structure, i.e. to also consider the imaginary parts of the refractive indices. Refractive index is a complex function, where the real part reflects the scattering, and the imaginary part reflects the absorption of the incident optical field in the medium.

The disadvantage is the extensive sequence of operations required on a small matrix. This greatly complicates the calculations. We will use complex refractive indices for layers in the form

$$\tilde{n} = n - ik. \quad \dots (1)$$

The transfer matrix method in optics is a mathematical technique used to analyze the propagation of light rays through an optical system by representing each optical element as a 2x2 matrix, allowing for the calculation of the ray's position and angle after passing through the entire system by multiplying these matrices together[22]. If the electromagnetic field is known at the beginning of a layer, the field at the end of the layer can be obtained from a simple matrix operation. The stack of layers can then be represented as a system matrix, which is the product of the matrices of the individual layers. The system matrices are then converted back into reflectance and transmittance. The absorptance is calculated from reflectance and transmittance.

According to TMM the optical characteristics of a multilayer structure can be represented by the 2×2 matrix[26]:

$$M_j = \begin{pmatrix} cos\delta_j & isin\delta_j/\gamma_j \\ i\gamma_j sin\delta_j & cos\delta_j \end{pmatrix}, \quad \dots (2)$$

where the phase angle is

$$\delta_j = \frac{2\pi}{\lambda}\left(\tilde{n}_j t_j \cos\theta_j\right). \quad \dots (3)$$

Here λ is the irradiation wavelength, j takes the values 1 and 2.

Because

$$det\, M_j = cos^2\delta_j + sin^2\delta_j = 1 \neq 0,$$

it can be argued that is not a singular matrix.

The quantity $\tilde{n}_j t_j \cos\theta_j$ is called the «effective optical thickness» of the layer for the angle of refractionθ_j, a$t_j$is the thickness of the corresponding j-th layer, and γ_j is "the effective refractive index", which, depending on whether the incident irradiation is polarized parallel or perpendicular to the plane of incidence, is given by

$$\gamma_j = \begin{cases} \tilde{n}_j/cos\,\theta_j \text{ parallel} \\ \tilde{n}_j \cos\theta_j \text{ perpendicular} \end{cases} \quad \dots (4)$$

In further computations, we accept perpendicularly polarized incident radiation to the surface of the structure.

According to the Descartes-Snell law for bordering media x and y with complex refractive indices n_x, n_y and k_x, k_y, we have[27]:

$$\frac{sin\theta_x}{sin\theta_y} = \frac{n_y}{n_x}\left[1 - \left(\frac{k_y}{n_y}\right)^2\right].$$

Usually the condition

$$\left(k_y/n_y\right)^2 \ll 1$$

is easily satisfied for the materials we use. This allows us to retain only the real parts of the refractive indices in the Descartes-Snell law, and to write the law as follows:

$$n_0 sin\theta_0 = n_2 sin\theta_2, n_2 sin\theta_2 = n_1 sin\theta_1. \quad \dots (5)$$

The overall optical behavior of the double layer structure presented in (Fig. 1) is represented by the product matrix M:

$$M = M_1 M_2 = \begin{pmatrix} m_{11} & m_{12} \\ m_{21} & m_{22} \end{pmatrix}. \quad \dots (6)$$

From Eqns. (2) and (6) we have:

$$\begin{pmatrix} cos\delta_1 & isin\delta_1/\gamma_1 \\ i\gamma_1 sin\delta_1 & cos\delta_1 \end{pmatrix}\begin{pmatrix} cos\delta_2 & isin\delta_2/\gamma_2 \\ i\gamma_2 sin\delta_2 & cos\delta_2 \end{pmatrix} = \begin{pmatrix} m_{11} & m_{12} \\ m_{21} & m_{22} \end{pmatrix},$$

$$\begin{pmatrix} cos\delta_1 cos\delta_2 + i\gamma_2 sin\delta_2\, isin\delta_1/\gamma_1 & cos\delta_1\, isin\delta_2/\gamma_2 + icos\delta_2 sin\delta_1/\gamma_1 \\ i\gamma_1 sin\delta_1 cos\delta_2 + i\gamma_2 sin\delta_2 cos\delta_1 & i\gamma_1 sin\delta_1\, isin\delta_2/\gamma_2 + cos\delta_1 cos\delta_2 \end{pmatrix} = \begin{pmatrix} m_{11} & m_{12} \\ m_{21} & m_{22} \end{pmatrix}, \quad \dots (7)$$

$\delta_j = \frac{2\pi}{\lambda}(\tilde{n}_j t_j \cos\theta_j) = \frac{2\pi}{\lambda}[(n_j - ik_j)t_j \cos\theta_j]$,
$\gamma_j = \tilde{n}_j \cos\theta_j = (n_j - ik_j)\cos\theta_j$.

Elements of the right side of the matrix (7) can be represented as the sum of real and imaginary parts as follows:

$m_{11} = m'_{11} + im''_{11}; m_{12} = m'_{12} + im''_{12}; m_{21} = m'_{21} + im''_{21}; m_{22} = m'_{22} + m''_{22}$.

After long and complex mathematical calculations for matrix elements m'_{ij} and m''_{ij} we obtain complicated expressions, which are presented below in the equation box. All the notations used in the calculations are also given there.

$m_{11} = m'_{11} + im''_{11}; m_{12} = m'_{12} + im''_{12}; m_{21} = m'_{21} + im''_{21}; m_{22} = m'_{22} + m''_{22};$

$m'_{11} = \epsilon_1\epsilon_4\Delta_1 - \epsilon_2\epsilon_3\Delta_2 - \sigma_1(\epsilon_1\epsilon_4\Delta_2 - \epsilon_2\epsilon_3\Delta_1) - \sigma_2(\epsilon_1\epsilon_2\Delta_4 + \epsilon_3\epsilon_4\Delta_3);$

$m''_{11} = \epsilon_1\epsilon_2\Delta_3 + \epsilon_3\epsilon_4\Delta_4 - \sigma_1(\epsilon_1\epsilon_2\Delta_4 + \epsilon_3\epsilon_4\Delta_3) + \sigma_2(\epsilon_1\epsilon_4\Delta_2 - \epsilon_2\epsilon_3\Delta_1);$

$m'_{12} = -\beta_1[n_1(\epsilon_1\epsilon_2\Delta_2 - \epsilon_3\epsilon_4\Delta_1) + k_1(\epsilon_1\epsilon_4\Delta_4 + \epsilon_2\epsilon_3\Delta_3)] - \beta_2[n_2(\epsilon_3\epsilon_4\Delta_2 - \epsilon_1\epsilon_2\Delta_1) + k_2(\epsilon_1\epsilon_4\Delta_3 + \epsilon_2\epsilon_3\Delta_4)];$

$m''_{12} = \beta_1[n_1(\epsilon_1\epsilon_4\Delta_4 + \epsilon_2\epsilon_3\Delta_3) - k_1(\epsilon_1\epsilon_2\Delta_2 - \epsilon_3\epsilon_4\Delta_1)] + +\beta_2[n_2(\epsilon_1\epsilon_4\Delta_3 + \epsilon_2\epsilon_3\Delta_4) - k_2(\epsilon_3\epsilon_4\Delta_2 - \epsilon_1\epsilon_2\Delta_1)];$

$m'_{21} = k_1\cos\theta_1(\epsilon_1\epsilon_4\Delta_4 + \epsilon_2\epsilon_3\Delta_3) - n_1\cos\theta_1(\epsilon_1\epsilon_2\Delta_2 - \epsilon_3\epsilon_4\Delta_1) - n_2\cos\theta_2(\epsilon_3\epsilon_4\Delta_2 - \epsilon_1\epsilon_2\Delta_1) + k_2\cos\theta_2(\epsilon_1\epsilon_4\Delta_3 + \epsilon_2\epsilon_3\Delta_4);$

$m''_{21} = k_1\cos\theta_1(\epsilon_1\epsilon_2\Delta_2 - \epsilon_3\epsilon_4\Delta_1) + n_1\cos\theta_1(\epsilon_1\epsilon_4\Delta_4 + \epsilon_2\epsilon_3\Delta_3) + n_2\cos\theta_2(\epsilon_1\epsilon_4\Delta_3 + \epsilon_2\epsilon_3\Delta_4) + k_2\cos\theta_2(\epsilon_3\epsilon_4\Delta_2 - \epsilon_1\epsilon_2\Delta_1);$

$m'_{22} = \epsilon_1\epsilon_4\Delta_1 - \epsilon_2\epsilon_3\Delta_2 - \sigma_4(\epsilon_1\epsilon_4\Delta_2 - \epsilon_2\epsilon_3\Delta_1) + \sigma_3(\epsilon_1\epsilon_2\Delta_4 + \epsilon_3\epsilon_4\Delta_3);$

$m''_{22} = \epsilon_1\epsilon_2\Delta_3 + \epsilon_3\epsilon_4\Delta_4 + \sigma_4(\epsilon_1\epsilon_2\Delta_4 + \epsilon_3\epsilon_4\Delta_3) + \sigma_3(\epsilon_1\epsilon_4\Delta_2 - \epsilon_2\epsilon_3\Delta_1);$

$\beta_1^{-1} = (n_1^2 + k_1^2)\cos\theta_1; \beta_2^{-1} = (n_2^2 + k_2^2)\cos\theta_2;$
$\beta_3 = \frac{2\pi}{\lambda}t_1\cos\theta_1; \beta_4 = \frac{2\pi}{\lambda}t_2\cos\theta_2;$

$2\epsilon_1 = e^{\beta_1 k_1} + e^{-\beta_1 k_1}; 2\epsilon_2 = e^{\beta_2 k_2} - e^{-\beta_2 k_2};$
$2\epsilon_3 = e^{\beta_1 k_1} - e^{-\beta_1 k_1}; 2\epsilon_4 = e^{\beta_2 k_2} + e^{-\beta_2 k_2};$

$\sigma_1 = \beta_1(n_1 n_2 + k_1 k_2)\cos\theta_2; \sigma_2 = \beta_1(n_1 k_2 - k_1 n_2)\cos\theta_2; \sigma_3 = \beta_2(n_1 k_2 + k_1 n_2)\cos\theta_1;$

$\sigma_4 = \beta_2(n_1 n_2 - k_1 k_2)\cos\theta_1;$

$\Delta_1 = \cos(\beta_3 n_1)\cos(\beta_4 n_2); \Delta_2 = \sin(\beta_3 n_1)\sin(\beta_4 n_2); \Delta_3 = \cos(\beta_3 n_1)\sin(\beta_4 n_2); \Delta_4 = \sin(\beta_3 n_1)\cos(\beta_4 n_2).$

The amplitudes of reflection and transmission coefficients r and $t$are given by the following expressions[22,23]:

$r = \frac{\gamma_0 m_{11} + \gamma_0 m_{12} - m_{21} - m_{22}}{\gamma_0 m_{11} + \gamma_0 m_{12} + m_{21} + m_{22}}, t = \frac{2\gamma_0}{\gamma_0 m_{11} + \gamma_0 m_{12} + m_{21} + m_{22}}.$

As a result

$r = \frac{+\gamma_0 m'_{12} - m'_{21} - m'_{22} + i(\gamma_0 m''_{11} + \gamma_0 m''_{12} - m''_{21} - m''_{22})}{\gamma_0 m'_{11} + \gamma_0 m'_{12} + m'_{21} + m'_{22} + i(\gamma_0 m''_{11} + \gamma_0 m''_{12} + m''_{21} + m''_{22})};$

$t = \frac{2\gamma_0}{\gamma_0 m'_{11} + \gamma_0 m'_{12} + m'_{21} + m'_{22} + i(\gamma_0 m''_{11} + \gamma_0 m''_{12} + m''_{21} + m''_{22})}.$

Here for air $\gamma_0 = n_0\cos\theta_0$.

The intensity of reflectance R and transmittance T are determined through the amplitudes r and t:

$R = |r|^2, T = \frac{\gamma_1}{\gamma_0}|t|^2.$

Then:

$R = \frac{(\gamma_0 m'_{11} + \gamma_0 m'_{12} - m'_{21} - m'_{22})^2 + (\gamma_0 m''_{11} + \gamma_0 m''_{12} - m''_{21} - m''_{22})^2}{(\gamma_0 m'_{11} + \gamma_0 m'_{12} + m'_{21} + m'_{22})^2 + (\gamma_0 m''_{11} + \gamma_0 m''_{12} + m''_{21} + m''_{22})^2},$ … (8)

$T = \frac{4\gamma_0\gamma_1}{(\gamma_0 m'_{11} + \gamma_0 m'_{12} + m'_{21} + m'_{22})^2 + (\gamma_0 m''_{11} + \gamma_0 m''_{12} + m''_{21} + m''_{22})^2}.$ … (9)

The absorptance A is defined as follows:

$A = 1 - R - T.$ … (10)

Absorption coefficient of DNA in the range 187-297 nm

In many theoretical problems related to the calculation of optoelectronic characteristics of bio-optical organic devices (sensors, receivers, emitters, *etc.*), it is necessary to have an analytical formula for the absorption coefficient α. The latter can be determined from the spectral dependence of absorptance A. Absorption coefficient can be calculated from this simple relation (see, Appendix):

$\alpha = 2.303\frac{A}{t},$ … (11)

Where t is the sample (DNA molecule) thickness.

Results and Discussion

As already noted, elastomeric PDMS ($n_1 = 1.4$, $k_1 = 10^{-6}$) is used as a substrate[18].

There is data in the literature on the technology of obtaining small values of the thickness of uniaxial nitrogen bases[9]. Following these studies, for numerical calculations we chose a real DNA thickness

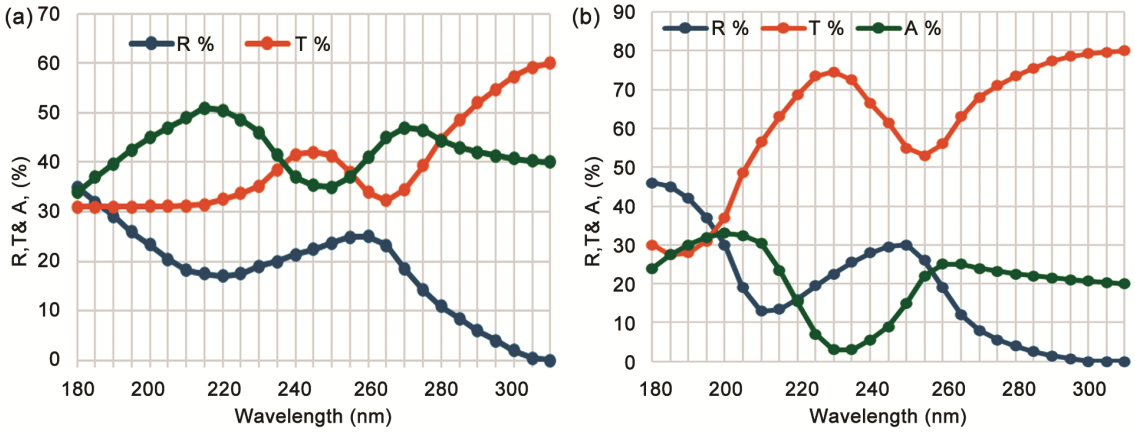

Fig. 2 — (a) Spectral dependency of reflectance, transmittance and absorptance of thin-layer DNA at the θ_0=30°; and (b) Spectral dependency of reflectance, transmittance and absorptance of thin-layer DNA at the θ_0=60°

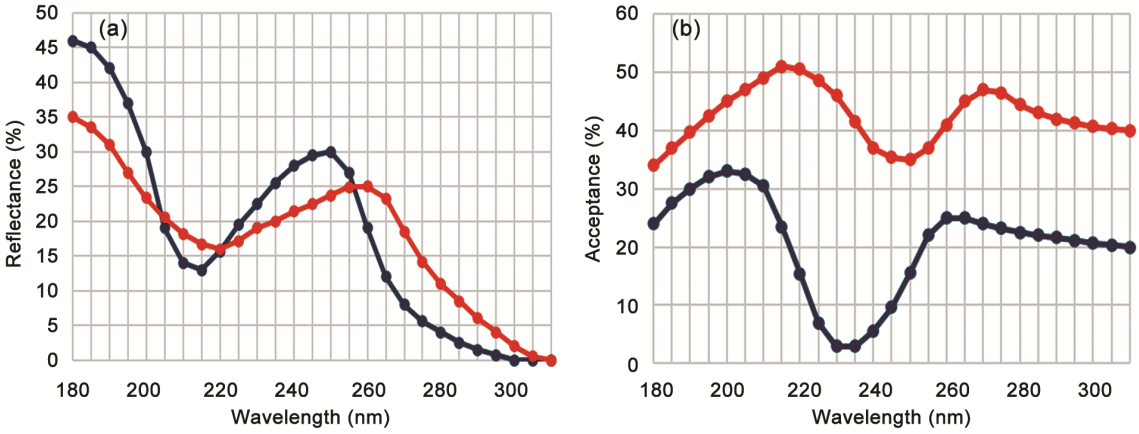

Fig. 3 — (a) Spectral dependence of reflectance. Blue curve is plotted for θ_0=30°, the red one for θ_0=60°; and (b) Spectral dependence of absorptance. Blue curve is plotted for θ_0=30°, the red one for θ_0=60°

of 10 nm. In the wavelength range 181-300 nm the real part the refractive indices of DNA molecules take values from 1.6 to 1.78 and imaginary part takes values from 0.27 to 0.052[12].

For numerical calculations in the wavelength range 180 - 310 nm we use the following parameters: $t_1 = 100$ nm, $t_2 = 10$ nm, $n_0 = 1$, $n_1 = 1.4$, $k_1 = 10^{-6}$. Two cases of incidence angle will be analyzed: $\theta_0 = 30°$ and $\theta_0 = 60°$. Numerical modeling was carried out in two cases:

- The case of averaged constant values of $n_2 = 1.68$ and $k_2 = 0.26$ for the considered spectral region of 180–310 nm (the results are presented in Figs. 2 and 3);
- The case considers the spectral dependence of $n_2(\lambda)$ and $k_2(\lambda)$ according to the data of Ref. [12] (the results are presented in Fig. 5).

The spectral dependences of reflectance and absorptance have a well-known behaviour with characteristic extrema (Figs. 2-5). Such extremes have been repeatedly detected experimentally[1,11-14]. As can be seen from (Fig. 2a), as expected, the behaviour of the absorptance almost mirrors the behaviour of the reflectance. This is seen more clearly on (Fig. 2b). The spectral dependence of the reflectance clearly shows a minimum (220 nm) and maximum (260 nm), which shift slightly towards short waves, correspondingly 215 nm and 250 nm with a decrease in the angle of incidence of irradiation (Fig. 3a). Clearly manifested extremes not only in behaviour, but also numerically completely coincide with experimental data[1,11-14].

At smaller angles θ_0 =30°, absorptance is shifted toward shorter wavelengths on ~15 nm: maximum from 215 and 270 nm shifted to 200 and 260 nm, minimum from 250 nm shifted to 233nm (Fig. 3b). Such weak shifts in the behavior of absorptance probably can be explained by the activation of excited

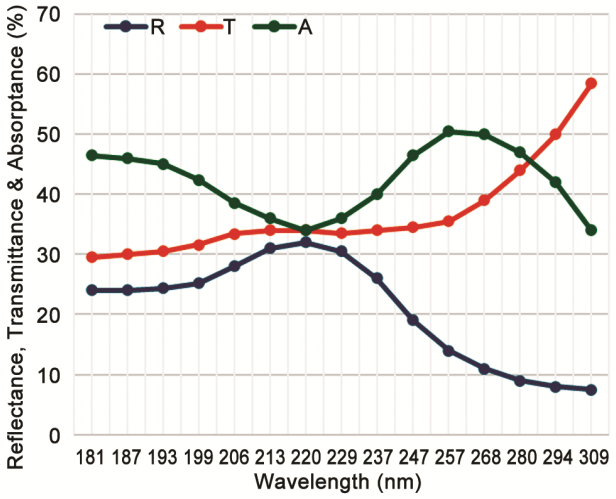

Fig. 4 — Spectral dependencies of reflectance, transmittance and absorptance at the θ_0=60° in the case of the spectral distribution of the refractive index of DNA

energy states HOMO and LUMO of DNA molecules (from 60° to 30°) and creating more favorable conditions for absorption of high-energy photons at the decreasing of incident irradiation angle. The dependence of the position of extreme points on the absorption spectrum on the angle of incidence of irradiation can be used to create an angle of incidence sensor. When DNA molecules are exposed to UV-B light, they absorb the light energy at a specific wavelength of around 200-220 and 250-260 nm.

Figure 4 shows the dependences $R(\lambda)$, $T(\lambda)$ and $A(\lambda)$ of a thin DNA film with a change in the refractive index of DNA according to the data[12], and at an incidence angle of 60°. Unlike Figures 2 and 3, the curves in (Fig. 4) are constructed using the spectral distribution of the real and imaginary parts of the DNA refractive index. The reflectance has a maximum at 220 nm, then decreases. Up to 257 nm absorptance exhibits almost mirror behaviour, passing through a minimum at 220 nm and taking a maximum value at 257 nm. The dependencies presented in (Fig. 4) do not change significantly when the angle of incidence of irradiation changes. Comparing the behaviour of the absorptance from (Fig. 3b and Fig. 4), for $\theta_0 = 60°$ we see that:

✓ Instead of two maximums in 213 nm and 270 nm there is one maximum in 257 nm, their absolute values are very close.

✓ Minimum in Figure 4 at 220 nm is very different from minimum in (Fig. 3b) (red curve, 250 nm). Their absolute values are very close.

It is obvious that the spectral dependency of absorptance presented in (Fig. 4) is more realistic and agrees quite well with the known experimental data presented in[1,11-14].

A comparison of the ratios of the amplitudes of the absorption maxima and minima shows a virtually complete match between our data (~1.56, Fig. 4) and the experimental data of work[13] (~1.67, Fig. 1) in work[13]. This confirms the acceptability of TMM for biomaterials.

Undoubtedly, the differences between curves in Figs. 3 and 4 is due to a change in the absorption spectrum. Such a shift of the extreme points is probably because the imaginary part of the refractive index for the upper curve in Fig. 3b (plotted at $k_2 = 0.26$) is comparatively greater than the imaginary parts of the refractive index for the minimum ($k_2 = 0.20$) and maximum ($k_2 = 0.12$) of the corresponding curve in Fig. 4. Since the $A(\lambda)$ has an ambiguous spectral dependence (Fig. 4), the modeling of dependency $\alpha(\lambda)$ is carried out as follows. Dividing the spectrum into two parts and using the extrapolation method, we construct the following dependencies:

a) Region with minimum acceptance at 220 nm

$$A_1(\lambda) = 0.34 + 20\left(\frac{\lambda}{220} - 1\right)^2;$$

$$\alpha_1(\lambda) = 2.3 \times 10^6 \left[0.34 + 20\left(\frac{\lambda}{220} - 1\right)^2\right]. \quad \ldots (12)$$

b) Region with maximum acceptance at 257 nm

$$A_2(\lambda) = 0.60 - 23.21\left(\frac{\lambda}{257} - 1\right)^2;$$

$$\alpha_2(\lambda) = 2.3 \times 10^6 \left[0.60 - 23.21\left(\frac{\lambda}{257} - 1\right)^2\right]. \quad \ldots (13)$$

In (12) and (13) the absorption coefficients are given in cm^{-1}. When obtaining formulas (12) and (13), the DNA layer thickness value of 10 nm was used and condition of equality of $\alpha_1(\lambda)$ and $\alpha_2(\lambda)$ is applied at the wavelength 237 nm. Total absorption coefficient α for wavelength diapason 190-290 nm will be the sum $\alpha_1(\lambda)$ and $\alpha_2(\lambda)$.

Figure 5 shows spectral dependency of absorption coefficient $\alpha(\lambda)$ of thin DNA layer. Its behavior is the same as absorptance behavior (Fig. 4, green curve). The magnitude of the absorption coefficient is quite large, which is due to the small thickness of the DNA layer.

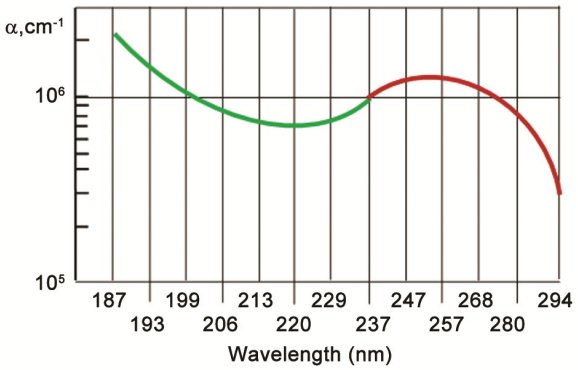

Fig. 5 — Spectral dependency of absorption coefficient. Green curve plotted according to (12), red one according to (13)

Conclusion

Theoretical simulation of optical properties of a two-layer structure containing a thin-layer DNA was performed using the TMM. The analysis was performed considering both the real and imaginary parts of the refractive index of the layers. Reflectance, transmittance and absorptance spectra were determined. In the case of constant average values of the real and imaginary parts of the refraction indices of DNA, the behavior of the reflection (absorption) coefficient, passing through a minimum (maximum) at the wavelength 215-220 nm and through a maximum (minimum) at 250-260 nm. When DNA molecules are exposed to UV light, they absorb light energy at specific wavelengths around 220 and 260 nm. In the case of considering the spectral distribution of the real and imaginary parts of the refractive index of DNA in the calculations, the behavior of the reflection and absorption coefficients shifts along the wavelength towards long waves: reflection has maximum value at 220 nm and then decreases tending to zero; absorptance have minimum value at 220 nm and maximum at 257 nm. It is shown that the position of the extreme points on the reflectance and absorptance is not only mutually related but also depends on the angle of incidence of the irradiation. An attempt was made to explain the spectral dependence of the absorptance of DNA both on the value of the imaginary part of the refractive index and on the initial angle of incidence of UV irradiation. Using the approximation method, on the base of spectral dependency of acceptance a formula is obtained for the DNA absorption coefficient for the wavelength range 185-295 nm. The correspondence between the behavior of reflectance and absorptance is generally consistent with known experimental data. The absorption of UV light at specific wavelengths provides important information that can be used in a variety of applications such as spectrophotometry and sensorics.

The results of this work can be used to create organic nanoscale biosensors for UV irradiation and nanoscale devices based on biomaterials. Intensive research is being conducted in this direction[1-6]. The results will also be useful in studying the optical properties and mechanisms of electric current transfer in various biomaterials.

Appendix

From the Beer-Lambert law we have:

$$\alpha t = \mathcal{T}n\left(\frac{I_0}{I}\right). \quad \text{(A1)}$$

Here I and I_0 are the intensities of transmitted and incident light, respectively, α is the absorption coefficient and t is the thickness of the thin layer. Acceptance A is decided as:

$$A \equiv log\left(\frac{I_0}{I}\right), \quad \text{(A2)}$$

or

$$A \equiv log\left(\frac{I_0}{I}\right) = ln\left(\frac{I_0}{I}\right) \times ln(e) = 0.4343 \times \alpha t.$$

Then

$$\alpha = 2.303\frac{A}{t}. \quad \text{(A3)}$$

By extending the Beer-Lambert law to a thin layer of DNA and assuming that it is a homogeneous medium, the absorption coefficient of DNA can be determined through the absorptance using formula (A3).

Acknowledgement

This research was funded by DNA-HIVE LLC.

Conflicts of interest

All authors declare no conflict of interest.

References

1 Yagura T, Makita K, Yamamoto H, Menck CFM & Schuch AP, Biological Sensors for Solar Ultraviolet Radiation. *Sensors*, 11 (2011) 4277.

2 Liang L, Fu Y, Wang D & Wei Y, DNA as functional material in organic-based electronics. *Appl Sci*, 8, (2018) 90.

3 Kwon YW, Lee CH, Choi DH & Jin JI, Materials science of DNA. *J Mater Chem*, 19 (2009) 1353.

4 Kawabe Y, Wang L, Horinouchi S & Ogata N, Amplified spontaneous emission from fluorescent-dye-doped DNA-surfactant complex films. *Adv Mater*, 12 (2000) 1281.

5 Gomez E, Steckl A, Irimia-Vladu M, Glowacki E, Sariciftci NS & Bauer S, Engineering DNA and nucleobases for present and future device applications. In the book*: Green Mater. Electron*. (Wiley-VCH Verlag GmbH & Co. KGaA) 2017, 191.

6 Muhammadi-Manesh E & Mir-Mahdevar M, Adsorption behavior of guanine, adenine, thymine and cytosine nucleobases of DNA on zinc oxide-graphene nanosensor: A DFT study. *Synth. Mat*, 267 (2020) 116486.

7 Prajzler V, Jung W, Oh K, Cajzl J & Nekvindova P, Optical properties of deoxyribonucleic acid thin layers deposited on an elastomer substrate. *Opt Mater Express*, 10 (2020) 421.

8 Singh R, Priye V & Chack D, Highly Sensitive Refractive Index-Based Sensor for DNA Hybridization Using Subwavelength Grating Waveguide. *IETE Tech. Rev*, 39 (2022) 1463.

9 Ghasemi M, Jeong H, Kim D, Kim B, Ik Jang J & Oh K, Linear and nonlinear optical properties of transfer ribonucleic acid (tRNA) thin solid films. *RSC Adv*, 12 (2022) 8661.

10 Pan X, Zhao Z & Zhang D. Characteristics of Azimuthal Seismic Reflection Response in Horizontal Transversely Isotropic Media under Horizontal in Situ Stress. *Surv Geophys,* 44 (2023) 387.

11 Samoc A, Miniewicz A, Samoc M & Grote JG, Refractive-Index Anisotropy and Optical Dispersion in Films of Deoxyribonucleic Acid. *Appl Polym Sci*, 105 (2007) 236.

12 Inagakit T, Hamm RN & Arakawa ET, Optical and dielectric properties of DNA in the extreme ultraviolet. *Chem Phys*, 61 (1974) 4246.

13 Kwon YW, Choi DH & Jin JI, Optical, electro-optic and optoelectronic properties of natural and chemically modified DNAs. *Polym. J,* 44 (2012) 1191.

14 Cavaluzzi MJ & Borer PN, Revised UV extinction coefficients for nucleoside-5¢-monophosphates and unpaired DNA and RNA. *Nucleic Acids Res*, 32 (2004) e13.

15 Sarantopoulou E, Kollia Z, Cefalas AC, Samardžija Z & Kobe S, Preparation of ultra-thin films of DNA bases with laser light at 157 nm. *TSF*, 495 (2006) 45.

16 Biedka S, Alkam D, Washam CL, Yablonska S, Storey A, Byrum SD & Minden JS, One-pot method for preparing DNA, RNA, and protein for multiomics analysis. *Commun. Biol*, 14 (2024) 324.

17 Jeong H & Oh K. Uracil-doped DNA thin solid films: a new way to control optical dispersion of DNA film using a RNA constituent. Opt. Express, 27 (2019) 36075.

18 https://refractiveindex.info/?shelf=organic&book=polydimethylsiloxane &page=Querry-NIR

19 Anzengruber SW, Klann E, Ramlau R & Tonova D, Numerical methods for the design of gradient-index optical coatings, *Appl. Opt*, 51 (2012) 8277.

20 Becker H, Tonova D, Sundermann M, Ehlers H, Günster S & Ristau D, Design and realization of advanced multi-index systems, *Appl. Opt*, 53 (2014) A88.

21 Luce A, Mahdavi A, Marquardt F & Wankerl H, TMM-Fast, a transfer matrix computation package for multilayer thin-film optimization: tutorial. *JOSAA*, 39 (2022) 1007.

22 Mackay TG & Lakhtakia A, The Transfer-Matrix Method in Electromagnetics and Optics. San Rafael, CA, Morgan and Claypool, 2020.

23 Han K & Chang CH, Numerical modeling of sub-wavelength anti-reflective structures for solar module applications. *Nanomaterials*, 4 (2014) 87.

24 Gasparyan F & Ayvazyan G, Reflection and Transmission of Radiation of the Structure Crystalline Silicon–Black Silicon–Perovskite. *J Contem Phys- Armen Acad Sci*, 57 (2022) 160.

25 Alamrani F & Alsharaeh E, Controlling the Bandgaps of One-Dimensional TiO_2/SiO_2, TiO_2/SnO_2, and SiO_2/SnO_2 Photonic Crystals Using the Transfer Matrix Method. *OPJ*, 12 (2022) 171.

26 Kuo ML, Poxson DJ, Kim YS, Mont FW, Kim JK, Schubert EF & Lin S-Y, Realization of a near-perfect antireflection coating for silicon solar energy utilization, *Opt Lett*, 33 (2008) 2527.

27 Kovalenko SA, Descartes-Snell law of refraction with absorption. *Semicond. Phys. Quantum Electron. Optoelectron*, 4 (2001) 214.